DOI: 10.1021/ma900314g

Macromolecules
ARTICLE

From Solutions to Membranes: Structure Studies of Sulfonated Polyphenylene Ionomers

Lilin He,[†] Cy H. Fujimoto,[‡] Chris J. Cornelius,[‡,§] and Dvora Perahia*[,†]

[†]*Department of Chemistry, Clemson University, Clemson, South Carolina 29634,* [‡]*Sandia National Laboratories, MS 0886, Albuquerque, New Mexico 87185-0886, and* [§]*Department of Chemical Engineering, Virginia Polytechnic Institute and State University, Blacksburg, Virginia 24061-0211*

Received February 11, 2009; Revised Manuscript Received August 1, 2009

ABSTRACT: The structure of rigid sulfonated polyphenylene ionomers was investigated in bulk and in dilute organic solutions. The uniqueness of polyphenylene ionomers lies in their rigid backbone which prevents folding and therefore affects the partition into hydrophilic ionic domains and hydrophobic regions. This segregation dominates the structure of flexible ionic polymers. Small-angle neutron scattering studies of these ionomers have demonstrated that bundles of polymer molecules are formed in dilute organic solutions. This clustered building block persists in bulk dry and hydrated states of the ionomers. Hydration of these ionomers membranes results in segregation to hydrophilic and hydrophobic regions, where diffusion into interstitial spaces between the bundles of sulfonated and unsulfonated domains takes place followed by rearrangements of domains to yield locally bicontinuous regions. Only at very high sulfonation levels are fully bicontinues phases formed. With controlling the degree of continuity, the stiffness of the backbone offers a means to tune the transport in ionic polymers.

1. Introduction

Ionomers are ion-containing polymers consisting of hydrophilic, ionizable side chains and a hydrophobic backbone.[1,2] They are used in a wide range of current and potential applications such as proton exchange membranes in fuel cells,[3] sensors,[4,5] electrochemical switches,[6] enzyme encapsulation,[7] and packaging materials.[8] In many of their applications, controlled transport of ions and solvents is required, where the formation of well-defined hydrophilic and hydrophobic regions tunes the dynamics within the ionomers.[9] Their technological significance resulted in a large number of studies that are primarily focused upon ionomers with semiflexible backbones.[10−12] Recently, it has been realized that the entire polymer structure, not only the ionic groups, affects the transport in ionic polymers. This realization led to an intensive synthetic effort to design new ionomers. Among these are polymers with a highly rigid backbone. The current study focuses on defining the structure of an ionic polymer that consists of a rigid polyphenylene backbone, whose stiffness affects the segregation into hydrophilic and hydrophobic domains, and the clustering of the ionic groups, the two driving forces that govern the structure of flexible ionomers.

Theoretical and experimental studies describe the segregation of the ionic groups in flexible polyemrs.[13−17] Eisenberg and co-workers formulated models that outline the balance between the energy of ionic clusters and the elasticity of the polymer.[10] These early models were further refined and adapted for specific systems.[14,16,18−21] The technological success in utilizing Nafion and its derivatives led to a plethora of studies.[10] Nafion consists of a perfluorinated backbone, substituted by hydrophilic side chains and terminated by sulfonic acid groups. Studies of Nafion solutions reveal that ionic interactions within and between polymer chains, together segregation into hydrophilic and hydrophobic parts, control its structure.[22] With hydrogen fuel cells and ion exchange membranes being among the most common applications of Nafion, in which the membranes are hydrated, the structural evolution of the polymers from dry materials to highly swollen and solutions was studied by several groups.[23−29] Gebel proposed a schematic phase diagram, describing the structural evolution of Nafion as a function of hydration level.[28] At low water content, the ionomer forms a structure of inverted micelle-like structure in which water is contained inside the ionic clusters. When the water volume fraction increases, the clusters swell and percolate to form bicontinuous structures[16] where this volume fraction depends on the specific ionomer. At significantly higher water content, "structure inversion" occurs, resulting in cylindrical hydrophilic water containing channels. Nafion eventually dissolves and form a connected network of rodlike particles. Schmidt Rohr and co-workers[29] have recently applied fast Fourier transform of space-filling models to distinguish various models proposed for the structure of Nafion. These studies concluded that within the humidity levels of ∼20 vol % water in Nafion, the structure is dominated by cylindrical water channels lying parallel to the polymer backbone, where the crystalline domains play a critical role in stabilizing the membranes.

Transport studies of Nafion have shown anisotropy in conductance which depends on the preparation method of these membranes. Gardner and co-workers[30] determined that the in-plane conductance of a Nafion 117 membrane is 0.0856 and 0.024 S/cm normal to it. These values are consistent with long cylindrical hydrated channels within the plane of the membrane as described by the Schmidt-Rohr model,[29] which are interconnected to allow transport, perpendicular to these channels, consistent with a degree of bicontinuity of the membranes.[11,16]

The present study investigates the structure of sulfonated polyphenylene (sPP) ionomers,[31−33] which consist of a highly rigid hydrophobic backbone with sulfonic acid functionalized phenyl side chains (Scheme 1). Modifying the rigidity of the backbone resulted in enhanced crystallinity and as such enhanced temperature stability, as shown for the predominantly *para* sPPs.[31]

*Corresponding author. E-mail: dperahi@ces.clemson.edu.

 Published on Web 08/19/2009

Scheme 1. Structural Formula of the Polyphenylenesulfonated Acid Ionomer Repeat Unit

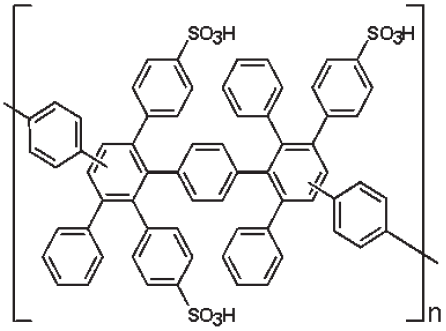

Table 1. Physical Parameters for the Ionomers[a]

IEC (mmol/g)	sulfonation level (%)
0.98	13.5
1.40	20.0
1.60	22.0
1.80	27.0
2.20	33.3
2.64	40.0
3.22	55.0

[a] IEC, or the ion exchange capacity, was determined by titration. Average molecular weight: 68 000 g/mol with polydispersity of 2.2.

The stereochemistry of the ionomer investigated in here is comprised of random distributions of *meta* and *para* repeat units that disrupt conjugation, leading to material that is soluble in organic solvents and processable into thin film as described by Fujimoto et al.[32] This ionomer was developed as an alternative to Nafion, and its chain flexibility and subsequent morphology are expected to differ from semiflexible polymers.[31−33] The structure of sPP ionomers was studied as a function of sulfonic acid concentration along the polymer backbone. Studies were carried out in dilute solutions and in hydrated thin films in order to explore their association characteristics as compared to semiflexible ionomers. These results present the first systematic studies of the factors that control the structure of highly rigid ionomers in an aqueous environment.

2. Experimental Section

2.1. Materials. The synthesis of sPPs was previously established.[32,33] Polyphenylene synthesized using 1,4-bis(2,4,5-triphenylcyclopendienone)benzene and 1,4-diethynylbenzene was postsulfonated using chlorosulfonic acid which yielded a randomly sulfonated ionomer, with M_w of 67 970 g/mol and polydispersity of 2.2, as expected from Diels−Alder polymerization.[32] T_g of the ionomers measured in this study is at ~320 °C. Further characterization data are given in ref 29. The characterization membranes with thickness of ca. 76 μm of sPP were made by evaporating a 10 wt % solution of sPP in the sodium form and *N,N*-dimethylacetamide (DMAc) from a glass plate. Their ion exchange capacity (IEC) determined by titration and the degree of sulfonation are listed in Table 1. The deuterium-labeled H_2O (99.9%) and tetrahydrofuran (THF) (99.5%) used for small-angle neutron scattering (SANS) were purchased from Cambridge Isotope Laboratories.

2.2. AFM Experiments. Tapping mode atomic force microscopy (AFM) was used to study the morphology of the surface of the membranes using a Multimode Nanoscope IIIa system and a multimode dimension 3000 Digital Instrument. Silicon nitride probes with 125 μm Olympus cantilevers, with a spring constant of 42 N/m and tip radius of less than 10 nm, were used at their fundamental resonance frequencies (280−350 Hz) at a scan rate of 1 Hz. Measurements were made under ambient conditions, room temperature and open to air, using a vibration isolation system, and image analysis was performed using Nanotech Software WSxM (version 4.1).

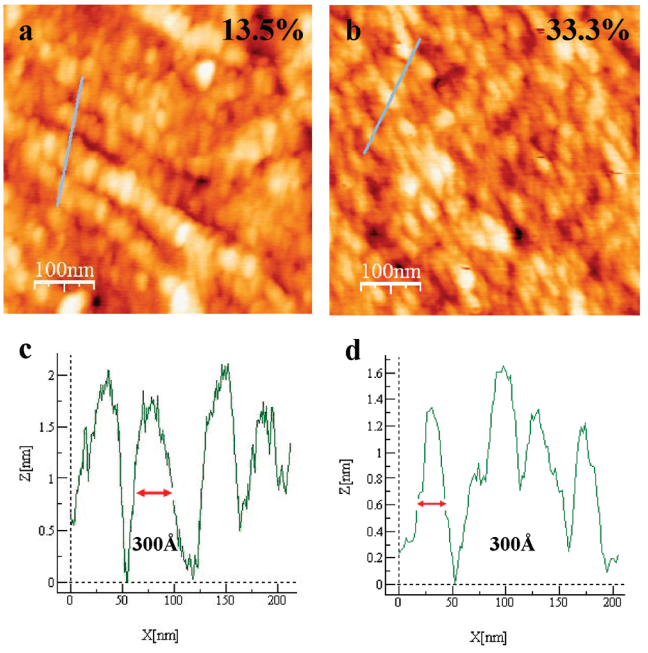

Figure 1. AFM topographic images of the membranes with sulfonation degrees of (a) 13.5% and (b) 33.3%. The corresponding depth profiles are shown in (c) and (d).

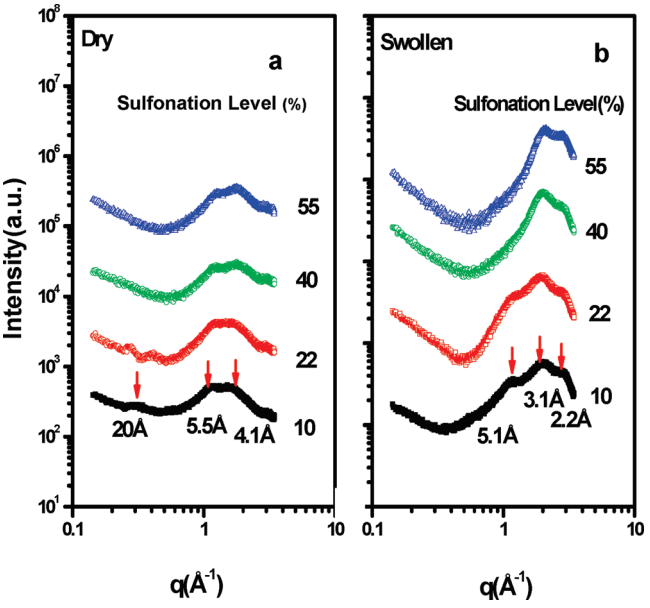

Figure 2. X-ray patterns of the ionomer membranes with different sulfonation degrees from 10% to 55%: (a) the membranes at dry state; (b) membranes at swollen state (patterns were shifted vertically for clarity).

2.3. X-ray Studies. X-ray scattering measurements were carried out in a reflection geometry on the thin films on a Sintag XDS200 powder diffractometer (Cu Kα, $\lambda = 1.54$ Å). Patterns were measured at 40 kV and 30 mA with a rectangular beam of 20 mm × 0.8 mm (width at half-maximum). The 2θ range for X-ray scattering was 2°−50°, where θ is the incident angle covering a q range of 0.14−3.45 Å^{-1}, where $q = 4\pi \sin \theta/\lambda$.

2.4. SANS Experiments. The SANS measurements were carried out at the Center for Neutron Research of the National institute of Standards and Technology (NIST) on the NG3 30 m

SANS at two detector distances, 13 and 1.5 m, with $\lambda = 6$ Å covering a q range from 0.0015 to 0.6 Å^{-1}. Measurements were performed on dry and swollen membranes as well as dilute solutions. The membranes were placed under vacuum overnight at room temperature to remove residual water from samples. Water uptakes of vacuum-dried membranes were separately measured to be between 3.5 and 4.5 wt %. Saturation, determined by separate gravimetrical measurements, was reached within the first 15 min of exposure to air at room temperature and room humidity. Dry membrane samples were capped in 2 mm thick titanium cells with quartz windows, for baseline measurements.[34] Water swollen membranes were allowed to equilibrate for 20 min prior to measurement. Independent water swelling studies were done with sPP between 25 and 60 °C which determined 20 min to be sufficient for achieving steady state for these materials.

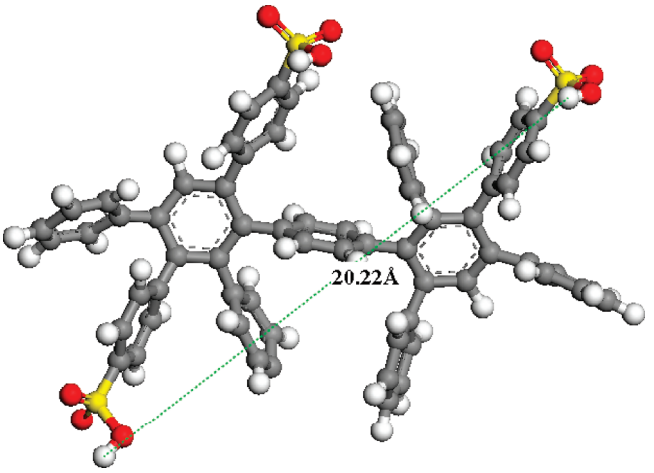

Figure 3. Conformation of two sPP units in vacuum obtained from molecular dynamics simulations using Accelrys' Material Studio software and polymer consistent force field (PCFF) with NVT ensemble at 298 °C. No changes are detected after 1 ns. The balls correspond to atoms: gray = carbon, white = hydrogen, yellow = sulfur, and red = oxygen.

Solutions were made by dissolving the powder samples in *d*-THF with concentrations ranging from 0.10 to 0.93 wt %. While the membranes were formed by evaporation of DMAc, *d*-THF was used to achieve contrast for SANS. The solvents were measured separately and subtracted from the data.

The data were collected at three different temperatures: 25, 40, and 55 °C. The temperature was controlled using a water bath to ±0.5 °C. The solvents were subsequently measured and subtracted from the data. Two-dimensional data were collected followed by integration into the one-dimensional patterns. The details of data reduction and data combining of two q ranges were given by NIST.[34]

3. Results and Discussion

3.1. Surface Morphology. Atomic force microscopy measurements were carried out on the surface of the membranes. Representative images for two sulfonation levels of 13.5% and 33.3% are shown in Figure 1. Surprisingly, relatively uniform domains ca. 150 Å in width and ca. 300 Å in length were observed. The long axis of the clusters line up in a given direction, whereas at lower sulfonation levels, further layering is observed. Since the membranes are not crystalline, as will be demonstrated using X-rays in Figure 2, the uniformity of the domains suggests that these are formed as a result of a self-assembly process that takes place as the solvent evaporates. The uniformity of these domains, considering the large molecular weight distribution of the polymers, is surprising. We attribute the regularity in domain sizes to the balance between hydrophobic and hydrophilic groups as well as the electrostatic forces.[9,13] Contact angle measurements have shown that the membranes are readily wetted by water and by hydrophobic solvents.[35] Therefore, the surface of the membrane and the clusters contain both hydrophilic and hydrophobic groups.

3.2. Structure Studies of the Membranes. Further studies exploring the internal structure of the membranes were carried out. X-ray patterns of the dry and hydrated membranes are shown in Figure 2. The X-ray patterns of the dry membranes (Figure 2a) exhibit several broad features that

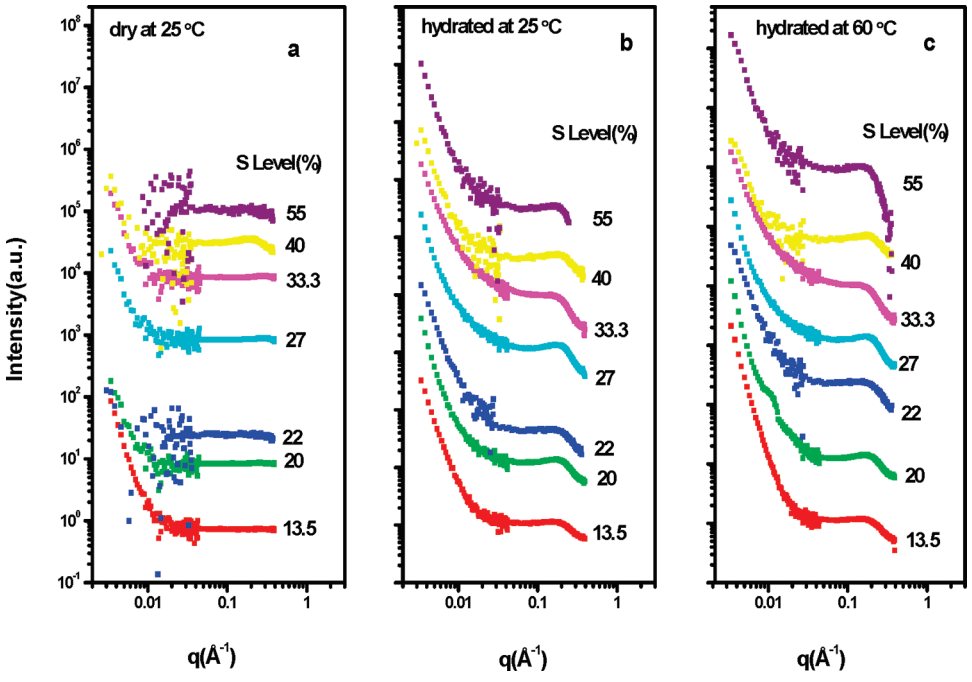

Figure 4. SANS profiles of the membranes at various sulfonation degrees from 10 to 55% at dry and hydrated states: (a) dry membranes at 25 °C, (b) hydrated membranes at 25 °C, and (c) hydrated membranes at 60 °C.

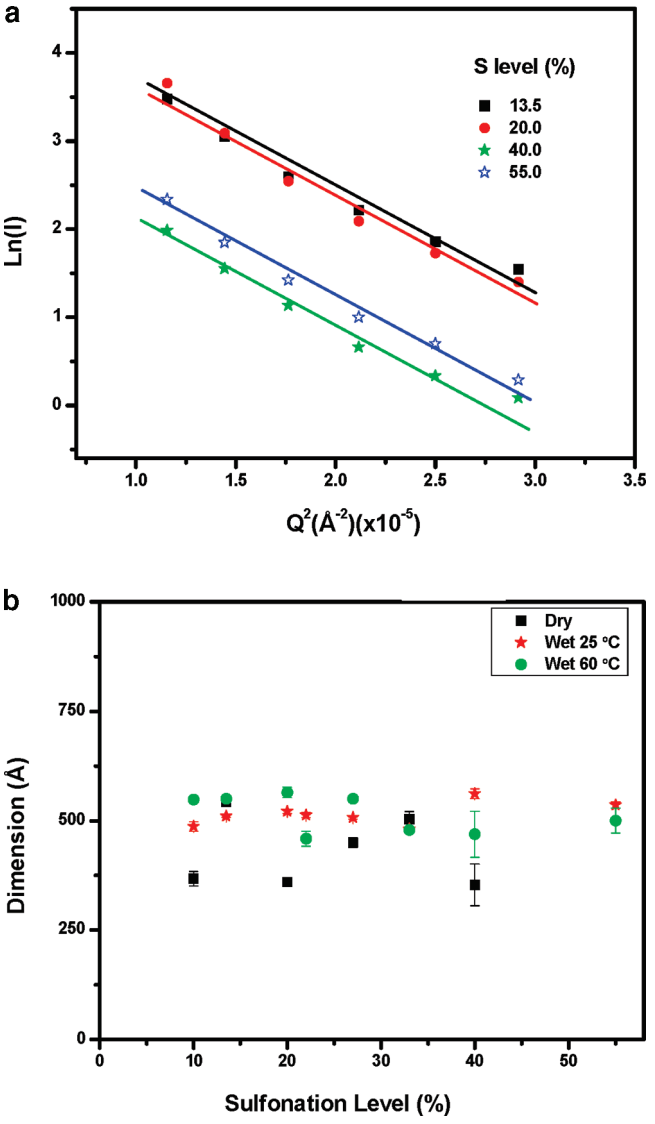

Figure 5. (a) Representative Guinier fits for four hydrated membranes at the indicated sulfonation levels at 25 °C. Experimental errors are within the size of the symbols. Best fit is defined with $R^2 \geq 0.97$. (b) Dimensions obtained from Guinier fits at low q range of the small-angle neutron scattering profiles as a function as sulfonation degree.

change slightly as sulfonation increases. A set of overlapping lines between q of 0.14 and 3.4 $Å^{-1}$ with two distinct peaks at 5.5 and 4.1 Å are observed together with a 20 Å line. The broad peak corresponds to average packing of different aromatic rings superimposed by intermolecular dimensions. The broad peak width is a result of the amorphous nature of the membranes. While Nafion is a semicrystalline polymer, no sharp peaks corresponding to crystalline domains are observed for sPP.

In order to evaluate the packing of the chains, the conformation of a single molecule of two sPP units in vacuum was calculated using molecular dynamic simulation as shown in Figure 3. This calculation shows that the aromatic rings on the backbone are not coplanar. Sterically, this is a lower energy configuration; however, it would disrupt close packing of the chains. This initial insight does not consider the solvent or neighboring polymer molecules; it does, however, offer a means to support the assignments of the X-ray lines. The origin of one feature, a peak at 20 Å, was not obvious. Its intensity was affected by the presence of solvent in the system. On the basis of the vacuum conformation of

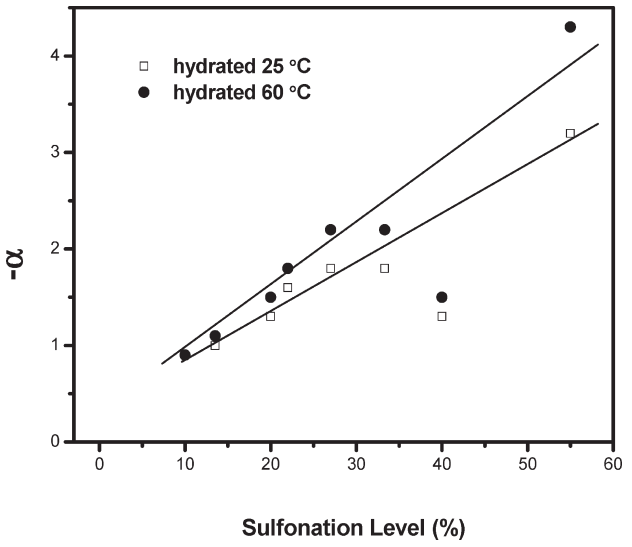

Figure 6. Index $-\alpha$ as a function as sulfonation degree for high q regime of hydrated membranes at 25 °C (open squares) and 60 °C (solid circles). The straight line represents the linear fit.

the sPP, this feature is assigned to the distance between two sulfonation groups within chains marked in Figure 3. Overall, the features are extremely broad, and the polymer chains assume multiple configurations. The introduction of more sulfonation groups results in disappearance of 20 Å line and hardly affects the aromatic region. The decrease in correlation between the sulfonated groups is attributed to the hydrophilic areas because of the water absorption.

As water diffuses into the sPP film, the patterns become slightly sharper and shift to higher q values (Figure 2b). The small changes observed upon hydration correspond to chain adjustments that take place as water penetrates and enhances slightly the mobility of the chains. However, the polymer remains predominantly disordered. For hydrated membranes, increasing sulfonation results in sharper peaks, and some of the molecular periodicities are not observed. The high q range has shown that though there is no tight $\pi-\pi$ stacking of the aromatic rings, they were correlated to form a hydrophobic domain, which is nonpenetrable to water. There were no dramatic changes in the overall structure reflected in the X-ray results as water penetrates.

X-ray provides the information on the length scale of 0.1−4 nm periodicities, which encapsulate inter- and intramolecular packing. Larger dimensions were probed by SANS. Figure 4 introduces the patterns of the dry and hydrated membranes at room and elevated temperatures. The dry membranes exhibit a significant amount of low-angle scattering that is characteristics of the large domains. This is consistent with AFM results that have recorded the existence of clustered polymers. Assuming that the cluster structure propagates throughout the membranes, the data were analyzed to obtain the average dimension using the Guinier approximation:[33]

$$I(q) = I(0) \exp(-q^2 R_g^2/3)$$

where $I(q)$ is the intensity of the scattering as a function of q, $I(0)$ is the intensity at $q = 0$, and R_g is the average radius of gyration of the cluster. Figure 5a shows the linear part of representative patterns and the relationship to fitting using Guinier approximation. The average R_gs determined from the slopes of the scattering patterns at low q are shown in Figure 5b. The dimensions of R_g for dry samples vary

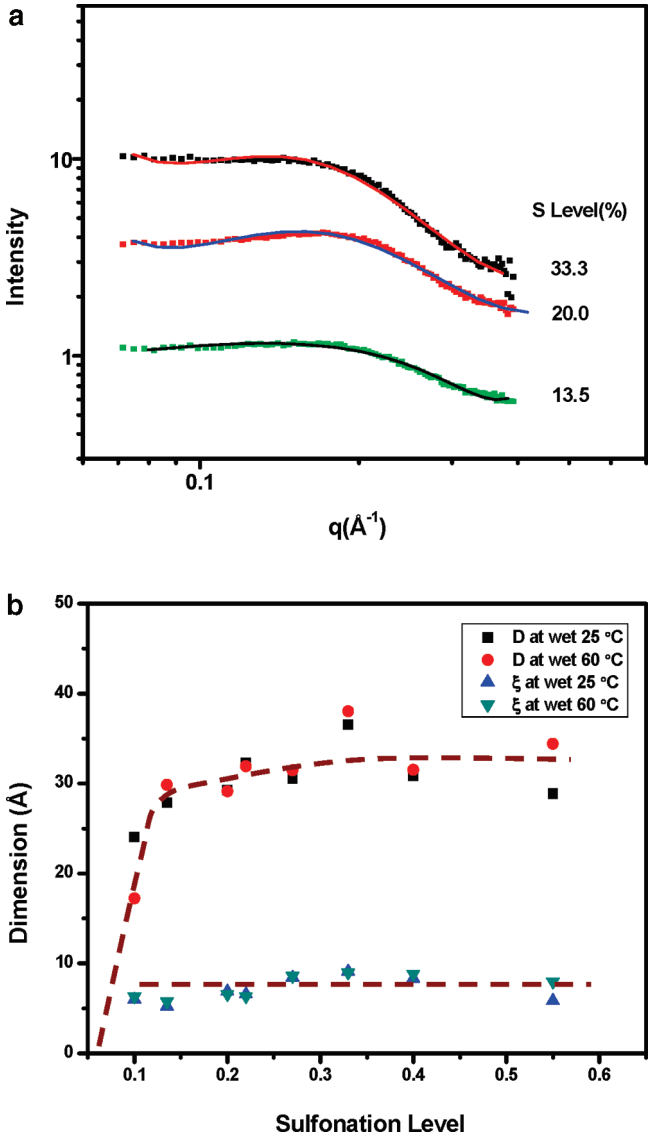

Figure 7. (a) Teubner−Strey model (full lines) of high q part of the SANS profiles from the membranes with three sulfonation levels (33.3, 20, and 13.5%). (b) Domain sizes and interdomain distances as a function as sulfonation level at different states. The data were obtained by fitting the high q part of SANS profiles at to Teubner−Strey bicontinuous model. D is interdomain distance, and ξ is correlation length.

between 350 and 540 Å. There is no obvious trend with sulfonation level.

In contrast to Nafion, the benchmark ionomer, there is no distinct peak that would correspond to hydrophilic domains. However, the AFM data combined with the X-ray and SANS are consistent with a membrane that is comprised of assemblies of bundles of polymers.

The membranes were exposed to D_2O at room temperature and at 60 °C. The patterns at different sulfonation levels are presented in Figure 4b,c. Similar to the dry membranes, the swollen membranes exhibit a rather strong low q scattering. While the slopes and the intensities of the patterns do not change, the signal-to-noise in this region improves significantly, which is potentially due to the enhanced contrast as D_2O penetrates into the interstitial space between the domains. A similar Guinier analysis was carried out, resulting in domain sizes of 460−560 Å. The range overlaps the dimensions observed for dry membranes. The similarity in

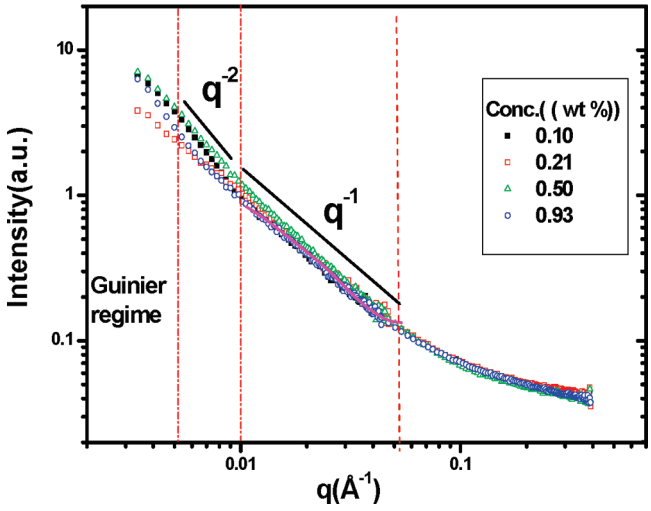

Figure 8. SANS profiles of solution sample with 13.5% sulfonation level at different concentrations. The solid line in the middle q range corresponds to a fitting to cylindrical aggregates.

domain sizes obtained for the dry and hydrated samples suggests that the water molecules penetrate in between cluster boundaries. The rigidity of the chains forces trapped ionic groups inside hydrophobic areas. These hidden groups offer a pathway for water molecules migrates into the domains at a later stage and change the structure.

With increasing hydration a peak develops at q ca. 0.2 Å^{-1}, corresponding to 32 Å in real space. While the low q regime shows almost no temperature dependence, the slope of the peak at higher q increases with increasing temperature, and its position is affected by the sulfonation level. The maximum of this line slightly shifts to lower q values with increasing sulfonation degree. The slopes were extracted from a fit of the tails of the peak to a linear line with R^2 of 0.96. The scattering intensity at high q range varies as q^{α} and α increases linearly from −0.9 to −4.0 with the sulfonation degree as shown in Figure 6. The slopes at 60 °C are higher than those at 25 °C as a result of formation of a smoother interface as more water penetrates.

For the semiflexible polymers such as Nafion and the Dow polymer, an analogue of Nafion with a perfluorinated backbone and a shorter side chain ($-OCHF_2CF_2SO_3H$), bicontinuous phases are formed as water penetrates into the membranes.[11,12] Note that transport measurements[30] and scattering models show that these bicontinuous phases would consist of preferential hydrophilic channels in the plane of the membranes interconnected to other direction.[11,16] A bicontinuous phase with sharp internal boundaries follows Porod's law.[36]

$$I(q) = (\Delta b)^2 \frac{2\pi}{q^4} S$$

Here Δb represents the scattering contrast and S the total internal surface. This relationship will hold for particles as well as nonparticulate systems if the internal surface is well-defined. The bicontinuous phase across the membrane will therefore express itself as a peak with a q^{-4} slope. In sPP ionomers, we observed slope as high as q^{-4} only at 60 °C for high ion content, which is consistent with the formation of a sharp interface in a bicontinuous network. As the sample swells, segregation into aqueous and hydrocarbon domains occurs, and the interfaces are defined by the sulfonic acid group domains. The broad line corresponds to the

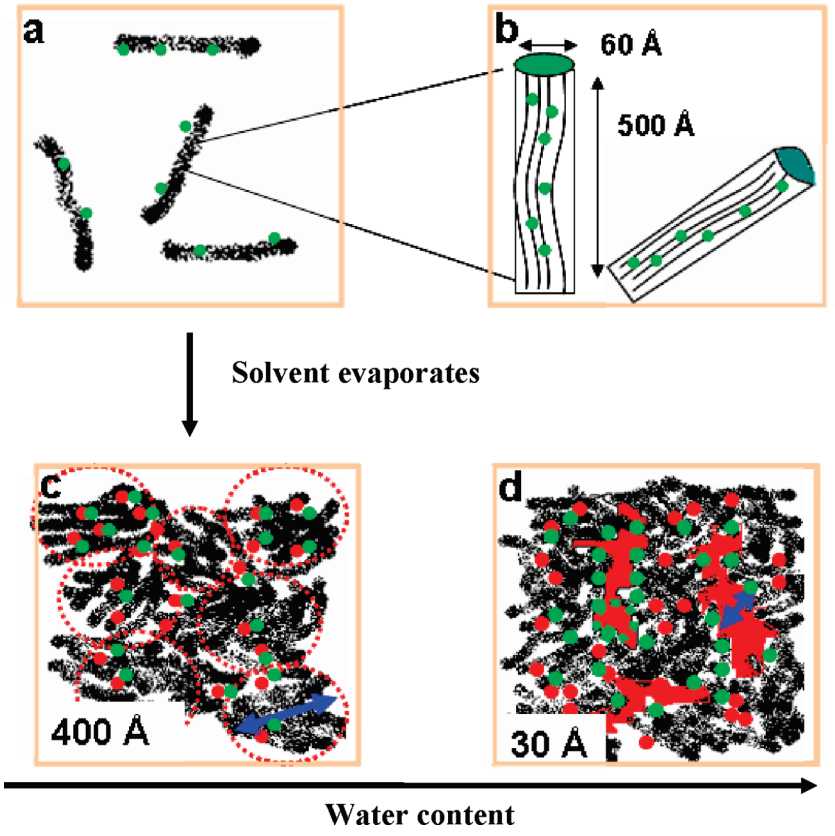

Figure 9. Schematic representation of the sPP ionomer from dilute solution to membrane. The rod represents the polymer backbone. The green sphere represents the sulfonic group, and the red sphere represents water molecule. (a) The ionomer in the dilute solution. (b) The dimension of the bundle of ionomers in solutions. (c) The dry membrane formation by the evaporation of the organic solvent and the dimension of the big aggregates is ca. 500 Å. (d) The fully hydrated membrane and the size of the hydrophilic areas is ca. 30 Å.

hydrophilic regions in analogous with semiflexible ionomers. Even though the degree of crystallinity is rather low, the hydrophobic domains support the film even at a very high hydration level despite the absence of physical cross-links.

The SANS patterns as a function of hydration of sPP do not exhibit the q^{-4} dependence, similar to Nafion, except over a very narrow sulfonation range at high humidity levels. This rigid ionomers however does locally segregates to hydrophilic and hydrophobic domains. This fact together with transport studies that have shown that the hydrophilic domains propagate across the membrane led us to describe the membranes in terms of *short-range bicontinuity*, with a well-defined internal surface. The data were fitted to the Teubner−Strey model that was developed for surfactant phases and used to describe in general two-component bicontinuous structures.[17,38] Based on Ginzburg−Landau theory, the model includes two characteristic length scales: interdomain distance d and correlation length ξ. A measure of the dispersion of the interdomain distance is measured by ξ. The fittings of three sulfonation levels are shown in Figure 7a. The d and ξ are described in Figure 7b. The interdomain distance increases with the sulfonation level while the dispersion remains constant. This provides further support to the assertion that this peak which developed as what penetrates is originated from the dimensions of the hydrophilic domain. The temperature hardly affects d and ξ. The invariance of d and ξ to temperature suggests at first the interstitial spaces. The size of the hydrophilic domains and the dispersion of the size remain the same.

3.3. Polymer Structure in Solution Studied by SANS. The membranes of sPP ionomers consists of bundles, as have been shown by AFM and SANS measurements. There regular size suggested that they were formed by self-assembly of the polymer as evaporation takes place. In order to probe the association of sPP association in a good solvent, the structure of dilute solutions of the polymer in THF using was studied. SANS profiles of sPP in d_6-THF with different concentrations are shown in Figure 8. At low q a slope of -2 is observed. A slope of -2 at low q would correspond to variety of structures. In this system, however, under the rigidity constraints of the backbone and the polydispersity of the polymer, the slope is consistent with an instantaneous formation of a network.[39] In the intermediate q region, the scattering exhibits a q^{-1} behavior over a limited q range, which is characteristic of elongated particles, indicating that the local shape of the aggregates is cylindrical. The crossover between the -2 and -1 slopes occurs at $q = 0.01$ Å^{-1}, which corresponds to dimension of ~630 Å. This dimension is consistent with molecular dimensions, where at higher q we zoom into the rigid part of the polymers. The curve was fit to the cylinder form factor:[36]

$$P(q) = \frac{L\pi}{q}\left[4\pi R^2\left(\frac{2J_1(qR)}{qR}\right)\right]^2$$

Here $J(x)$ is first order of Bessel function, and R and L are the radius and length of the rod, respectively. A radius with a dimension of 60 ± 5 Å and a length with dimension of 500 ± 20 Å were obtained. The radius of a single rodlike molecule in solution is ca. 20 Å. A larger radius is a clear indication that even in low concentrations bundles are formed. Similar to the structure in the solid membrane, the structure in solution is independent of temperature in the range of 25−55 °C.

A schematic model that describes the association of the polymers and hydration of the membranes is shown in Figure 9. In dilute organic solutions, the elongated bundles made of packed and aligned polymer chains with the pendant sulfonated groups located at the periphery (Figure 9 top). With increasing polymer concentration, a loose network structure is formed. As the solvent evaporates, the bundles that dominate solution structure further associate to form membranes. Large polymeric aggregates with dimension of ~400 Å are depicted, resulting from the balance between hydrophobic and hydrophilic groups as well as the electrostatic forces.

When placed in an aqueous environment, the membrane takes up water. Some water molecules associated with the sulfonic groups, and some are dispersed in the polymer matrix. With increasing the water content, water molecules penetrate into hydrophilic sites and form clusters with dimension of ca. 30 Å, where the bundle structure is retained. The rigidity of the backbone results in buried hydrophilic moieties within bundles. With increasing temperature and hydration time, enhanced mobility of the chains allows penetration of water into some of the bundles. Eventually the hydrated membranes form locally bicontinuous regions (Figure 9, bottom).

4. Conclusions

The current study elucidated the structure of a rigid sPP ionomers in organic solutions and in dry and hydrated membranes. Bundles or rodlike aggregates dominate the solution structure as well as that of the membranes. When hydrated, the water first penetrates in between these structures followed by rearrangements and eventual formation of local bicontinuous structures. Similar to flexible ionic polymers, these rigid ionomers associate. The rigidity of the backbone, however, affects the degree of phase segregation into hydrophilic and hydrophobic parts. As a result, the macroscopic structure of the ionic membrane, or the degree of propagation of the bicontinuity, differs from that of flexible ionomers. Consequently, controlling the rigidity of the backbone of ionomers offers a means to modify the available transport pathways in ionomers.

Acknowledgment. We acknowledge the support of the National Institute of Standards and Technology, U.S. Department of Commerce, and Lujan Center at LANL in providing the neutron research facilities used in this work and Sandia National Laboratories for funding and materials. The authors also thank Sabina Maskey for her simulation work and Thusitha Etampawala for his help with the membrane swelling experiment. Sandia is a multiprogram laboratory operated by Sandia Corporation, a Lockheed Martin Co., for the United States Department of Energy's National Nuclear Security Administration under Contract DE-AC04-94AL85000. DOE Grant DE-FG02-07ER46456 is acknowledged for supporting this work.

References and Notes

(1) Pineri, M.; Eisenberg, A. *Structure and Properties of Ionomers*; D. Reidel Publishing Co.: Dordrecht, Holland, 1987; p 291.
(2) Schlick, S. *Ionomers: Characterization, Theory and Applications*; CRC Press: Boca Raton, FL, 1996; p 3.
(3) Truffler-Boutry, D.; Geyer, A. D.; Diat, O.; Gebel, G. *Macromolecules* **2007**, *40*, 8259.
(4) Ugo, P.; Moretto, L. M.; Vezzà, F. *ChemPhysChem* **2002**, *3*, 917.
(5) Whiteley, D. L.; Martin, C. *Anal. Chem.* **1987**, *59*, 1746.
(6) Nilsson, D.; Kugler, T.; Svensson, P. O.; Berggren, M. *Sens. Actuators, B* **2002**, *86*, 193.
(7) Flarrison, J. D.; Turner, F. B. R.; Baltes, B. H. *Anal. Chem.* **1988**, *60*, 2002.
(8) Maki, N.; Tajitsu, Y.; Sasaki, H. *Packag. Technol. Sci.* **2007**, *20*, 309.
(9) Lantman, C. W.; MacKnight, W. J. *Annu. Rev. Mater. Sci.* **1989**, *19*, 295.
(10) Mauritz, K. A.; Moore, R. B. *Chem. Rev.* **2004**, *104*, 4535.
(11) Kreuer, K. D. *J. Membr. Sci.* **2001**, *185* (1), 29.
(12) Serpico, J. M.; Ehrenberg, S. G.; Fontanella, J. J.; Jiao, X.; Perahia, D.; McGrady, K. A.; Sanders, E. H.; Kellogg, G. E.; Wnek, G. E. *Macromolecules* **2002**, *35*, 5916.
(13) Eisenberg, A. *Macromolecules* **1970**, *3*, 147.
(14) Eisenberg, A.; Hird, B.; Moore, R. B. *Macromolecules* **1990**, *23*, 4098.
(15) Essafi, W.; Gebel, G.; Mercier, R. *Macromolecules* **2004**, *37*, 1431.
(16) Gierke, T. D.; Munn, G. E.; Wilson, F. C. *J. Polym. Sci., Polym. Phys. Ed.* **1981**, *19*, 1687.
(17) Roche, E. J.; Pineri, M.; Duplessix, R.; Levelut, A. M. *J. Polym. Sci., Polym. Phys. Ed.* **2003**, *19*, 1.
(18) Macknight, W. J.; Taggart, W. P.; Stein, R. S. *J. Polym. Sci., Polym. Symp.* **1974**, *45*, 113.
(19) Forsman, W. C. *Macromolecules* **1982**, *15*, 1032.
(20) Dreyfus, B. *Macromolecules* **1985**, *18*, 284.
(21) Gouin, J. P.; Williams, C. E.; Eisenberg, A. *Macromolecules* **1989**, *22*, 4573.
(22) Aldebert, P.; Dreyfus, B.; Gebel, G.; Nakamura, N.; Pineri, M.; Volino, F. *J. Phys.* (*Paris*) **1988**, *49*, 2101.
(23) Loppinet, B.; Gebel, G. *Langmuir* **1998**, *14*, 1977.
(24) Gebel, G.; Loppinet, B.; Hara, H.; Hirasawa, E. *J. Phys. Chem. B* **1997**, *101*, 3980.
(25) Hara, M.; Wu, J.; Lee, A. H. *Macromolecules* **1989**, *22*, 754.
(26) Szajdzinskapietek, E.; Pilar, J.; Schlick, S. *J. Phys. Chem.* **1995**, *99*, 313.
(27) Loppinet, B.; Gebel, G.; Williams, C. E. *J. Phys. Chem. B* **1997**, *101*, 1884.
(28) Gebel, G. *Polymer* **2000**, *41*, 5829.
(29) Schmidt-Rohr, K.; Chen, Q. *Nat. Mater.* **2008**, *7* (1), 75.
(30) Gardner, C. L.; Anantaraman, A. V. *J. Electroanal. Chem.* **1998**, *449*, 209.
(31) Litt, M.; Granados-Focil, S. *PMSE Prepr.* **2006**, *95*, 138.
(32) Fujimoto, C. H.; Hickner, M. A.; Cornelius, C. J.; Loy, D. A. *Macromolecules* **2005**, *38*, 5010.
(33) Cherry, B. R.; Fujimoto, C. H.; Cornelius, C. J.; Alam, T. M. *Macromolecules* **2005**, *38*, 1201.
(34) http://www.ncnr.nist.gov/programs/sans/equipment/banj_cell.html.
(35) He, L.; Smith, H. L.; Majewski, J.; Fujimoto, C. H.; Cornelius, C. J.; Perahia, D. *Macromolecules* **2009**, *42*, 5745.
(36) Kline, S. R. *J. Appl. Crystallogr.* **2006**, *39*, 895.
(37) Glatter, O.; Kratky, O. *Small Angle X-ray Scattering*; Academic Press: New York, 1982.
(38) Teubner, M.; Strey, R. *J. Chem. Phys.* **1987**, *87*, 3195.
(39) Schubert, K.-V.; Strey, R.; Kline, S. R.; Kaler, E. W. *J. Chem. Phys.* **1994**, *101*, 5343.